Allocation of EV Public Charging Station in Renewable based Distribution Network using HHO Considering Uncertainties and Traffic Congestion

Arnab Pal
National Institute of Technology Agartala
Aniruddha Bhattacharya (bhatta.aniruddha@gmail.com)
National Institute of Technology Durgapur https://orcid.org/0000-0002-4059-1090
Ajoy Kumar Chakraborty
National Institute of Technology Agartala

Research Article

Keywords: Distributed generation, EV charging station, HHO, optimal allocation, 2m PEM, uncertainty

Posted Date: May 7th, 2021

DOI: https://doi.org/10.21203/rs.3.rs-172433/v1

Allocation of EV Public Charging Station in Renewable based Distribution Network using HHO Considering Uncertainties and Traffic Congestion

Arnab Pal[1], Aniruddha Bhattacharya[2,*], Ajoy Kumar Chakraborty[1]
[1]Department of Electrical Engineering, National Institute of Technology Agartala, India
[2]Department of Electrical Engineering, National Institute of Technology Durgapur, India
arnabpal1994@gmail.com; bhatta.aniruddha@gmail.com; akcall58@gmail.com
* Corresponding author

***Abstract*—Electric vehicle (EV) is the growing vehicular technology for sustainable development to reduce carbon emission and to save fossil fuel. The charging station (CS) is necessary at appropriate locations to facilitate the EV owners to charge their vehicle as well as to keep the distribution system parameters within permissible limits. Besides that, the selection of a charging station is also a significant task for the EV user to reduce battery energy wastage while reaching the EV charging station. This paper presents a realistic solution for the allocation of public fast-charging stations (PFCS) along with solar distributed generation (SDG). A 33 node radial distribution network is superimposed with the corresponding traffic network to allocate PFCSs and SDGs. Two interconnected stages of optimization are used in this work. The first part deals with the optimization of PFCS's locations and SDG's locations with sizes, to minimize the energy loss and to improve voltage profile using harris hawk optimization (HHO) and few other soft computing techniques. The second part handles the proper assignment of EVs to the PFCSs with less consumption of the EV's energy considering the road distances with traffic congestion using linear programming (LP), where the shortest paths are decided by Dijkstra's algorithm. The 2m point estimation method (2m PEM) is employed to handle the uncertainties associated with EVs and SDGs. The robustness of solutions are tested using wilcoxon signed rank test and quade test.**

***Index Terms*—Distributed generation, EV charging station, HHO, optimal allocation, 2m PEM, uncertainty.**

I. Introduction

Use of EV is the way to replace the conventional fossil fuel-based vehicle and it helps to reduce the carbon emission and fossil fuel consumption (Wei et al. 2019). Nowadays, the number of users is rapidly increasing who are motivated towards the EV. However, the availability of public charging station is one of the important hesitations to adopt EV. Therefore, the fast charging station is the greatest solution for the public charging infrastructure (Sadeghi-Barzani et al. 2014; Motoaki 2019), which needs to be allocated optimally. The PFCS creates enormous load to the power system network which leads to huge power loss and makes the voltage profile weaken. Therefore, appropriate allocation of PFCSs is very crucial to keep the losses minimum with a healthy voltage profile. Moreover, the improper selection of PFCS by the EV owners can cause extra energy consumption of batteries to reach at CS, which affects the energy demand from the power system.

The suitable locations are selected for CS in (Zhang et al. 2019a), based on service risk parameter using upgraded whale optimization technique. Authors in (Wang et al. 2013), allocated the CS in a distribution network overlapped with traffic network where the objectives are minimization of the power loss and voltage deviation. The fast-charging stations are allocated in a test system to minimize the various costs including losses in (Sadeghi-Barzani et al. 2014). The total cost is minimized in (Liu et al. 2013) by optimal siting and sizing of the CSs in IEEE 123 distribution system with reduced power loss and improved voltage profile. In (Awasthi et al. 2017), the optimal locations are identified in the distribution network of Allahabad city for electric vehicle charging station (EVCS) to minimize the active power loss and development cost. Real power loss is minimized in (Pal et al. 2019; Ponnam and Swarnasri 2020) to CS in radial distribution network using several soft-computing techniques. In (Zhang et al. 2019b), the cost for the CS is minimized with maximum service capability by the optimal allocation in Beijing city. Optimal battery swapping stations are planned in IEEE 15 bus distribution system in (Zheng et al. 2014). In (Davidov and Pantoš 2019), the placement cost of the CS is minimized considering the power system reliability constraints. Authors in (Liu et al. 2020) considered annual profit maximization to allocate DG and EVCS in 33 and 69 distribution system. In (Shaaban et al. 2019; Luo et al. 2020) CS and DG are optimally allocated in a micro-grid and distribution network respectively considering the cost minimization. Simultaneous allocation of CS and DG is proposed in (Atat et al. 2020) with charging coordination. Location and capacity of CSs are optimized considering user satisfaction in (Yi et al. 2019). Charging stations' locations are found out in (Gong et al. 2019) based on millage and distribution of EVs. CSs are allotted with different charging level and various associated costs are minimized in (Liu and Bie 2019). The uncertain driving pattern is taken during allocation of CS with minimum cost in (Andrade et al. 2020). The locations of CS are found out in IEEE 69 distribution system with optimal grid to vehicle (G2V) and vehicle to grid (V2G) scheduling in (Hadian et al. 2020). (Xiong et al. 2018; Dong et al. 2019; Hosseini and Sarder 2019; Kong et al. 2019) provide good solutions to allocate the CS in geographical map and road network. In (Spieker et al. 2017), multi-objective is solved

using a modified genetic algorithm to serve maximum number of EV by placing EVCS. The optimal charging facilities are selected in (Wu et al. 2020) considering uncertainties. Uncertain vehicle rent is taken care for maximum profit of suppliers in (Long et al. 2019).

Research work on charging station allocation are still limited. The major shortfalls from most of the available articles are, either CSs are allocated in power system network or in road network. Moreover, a very few tackled the uncertainties of EV flow and state of charge (SOC) requirement. The EVs need to be assigned at right CS by using minimum battery energy to travel up to CS, to reduce the energy demand from the power system. As per best knowledge of the authors, the apt selection of the CS by the EVs considering road congestion is not considered in the existing literatures while dealing with PFCS allocation. However, the CSs also should be distributed in the area to serve all the EV users effectively. Furthermore, the EV's motivation regarding air pollution reduction would not be satisfied if the EV takes power, generated by conventional power plants, during charging process. Therefore, the power system should be renewable supported installed with optimal sizes and locations. Again, the EV flow, PV output and loads are having hourly variations. Therefore, power loss minimization as considered in most of the papers is not proper for a sustainable solution because energy loss minimization is more justified in a dynamic environment.

In this present work, the energy loss minimization is adopted as objective to decide the optimal locations of PFCS and locations along with sizes of SDG in the distribution network. The solar-based DGs are incorporated to reduce the energy loss and to improve the voltages with less carbon emission.

A superimposed network with a distribution system and road map is taken as the study area. Three zones are considered in the study area to allocate the PFCSs in distributed pattern which will help to serve all users evenly. The solution methodology is proposed in two interconnected stages. In the first stage, the PFCSs are allocated and SDGs are located with their optimal sizes simultaneously. The second stage works to assign the EVs at apt PFCS and helps to calculate the load and energy demand at respective PFCSs. HHO and Grey wolf optimizer (GWO) are used in first stage and the energy loss is minimized. Finally, eight other optimization techniques are also used to validate the solutions. In the second stage, the integer linear programming (ILP) is clubbed to find out the suitable PFCS for the EVs to minimize their energy requirement. The traffic congestion and distance which affect the SOC of the EV to reach up to the PFCS, both are taken into account to choose the apt CS for the EVs with minimum energy requirement. The shortest routes are found out by the Dijkstra's algorithm. The annual average 24 hours' variations of EV flow, PV profile and conventional load profile are taken in this work. Moreover, instead of fixed random values, the uncertainties related to SOC requirements, EV locations, traffic congestions and solar irradiance, are handled by a powerful statistical tool, i.e. 2m PEM.

In brief, the key contributions of the paper are: 1) Energy loss minimization instead of power loss minimization considering dynamic event, 2) Placement of PFCSs in a superimposed network with power distribution system and traffic network, 3) Zone wise allocation of PFCS to make it distributed in the area, 4) Simultaneous allocation of SDGs to reduce the energy loss and to improve voltage profile, 5) Proper assignment of EVs at PFCSs considering the shortest distance with traffic congestions, 6) Consideration of all possible uncertainties associated with EV, SDG and traffic congestion using 2m PEM. The statistical hypothesis tests i.e. wilcoxon signed rank test and quade test, are performed to check robustness of the solutions and to confirm the hypothesis.

The rest of this article is arranged as follows. Section II shows the modelling and formulation for both the stages with constraints. Section III presents the solution methodologies to solve the problem, i.e. HHO, 2m PEM and algorithm of the entire procedure. The results and discussion are demonstrated in section IV. This paper is concluded in section V with a roundup and future possibility.

II. Mathematical Formulation

The entire problem is formulated in two stages interconnected with each other. In the first stage, the energy loss is minimized by optimal allocation of PFCSs and SDGs. In the second stage, the EVs reach to apt PFCS by spending minimum energy. The SOC arrival and first trip distance in the first stage depend on the second stage after assigning the EV at apt PFCS.

A. Stage I: Allocation of PFCS and SDG

The main objective in this stage is to keep the energy loss minimum by allocating the PFCS at optimal places. Moreover, the optimal locations and sizes of the SDG need to find out based on the same objective to reduce more loss. The objective function, constraints, load modelling and energy requirements are discussed below.

1) Objective Function-1 (F_1)

$$F_1 = min\left\{\sum_{t=1}^{T}\sum_{br=1}^{N_{br}} R_{br}\cdot\frac{P_{br}^2(t)+Q_{br}^2(t)}{V_{br}^2}\right\} \quad (1)$$

where $P_{br}(t)$ and $Q_{br}(t)$ are real and reactive power flow through br^{th} branch respectively at t^{th} time, V_{br} is voltage of the sending node of br^{th} branch, R_{br} is resistance of branch br. T and N_{br} are total time interval and total number of branch respectively.

2) Constraints

The voltage of every node at any time interval should be within permissible limits as presented in (2), where V_{min} and V_{max} are the lower and upper limits respectively.

$$V_{min} \le V_{br}(t) \le V_{max}, \qquad \forall\, br, t \quad (2)$$

The current flowing through every branch (I_{br}), should be less than the allowable upper limit (I_{max}).

$$|I_{br}| \le I_{max}, \qquad \forall\, br \quad (3)$$

The total installed capacity of the SDGs should not be more than the DG penetration level (λ_p) as follows.

$$\sum_{dg=1}^{N_{dg}} IC_{dg} \le \lambda_p \cdot load_p \quad (4)$$

where $load_p$ is the peak load of the system and IC_{dg} is the installed capacity of the dg^{th} SDG.

The power generated from SDGs (P_{sdg}) and power supplied from the utility (P_{ut}) should be equal to total load (L_T) and

total loss ($Loss_T$) at any hour t^{th}. Therefore, the load balancing constraint is written as:

$$P_{sdg}(t) \cup P_{ut}(t) \in L_T(t) \cup Loss_T(t), \forall\, t \quad (5)$$

Branch thermal limit constraint is provided bellow.

$$|S_{br}| \leq |S_{br}^{max}|, \quad \forall\ br \quad (6)$$

where S_{br} is apparent power of branch br and S_{br}^{max} is the maximum apparent power limit of br^{th} branch.

Zone constraint is taken in consideration to make the public charging station (g) distributed over the city. This will bound one PFCS in each zone.

$$g_i \in \mathbb{Z}_i, i \in no.of\ zone \quad (7)$$

where S_i is the i^{th} EVCS and $\mathbb{Z}_i$ is the i^{th} zone.

The maximum SOC level (SOC_{max}) and minimum SOC level (SOC_{min}) should be maintained to keep the battery healthy.

$$SOC_{min} \leq SOC_h \leq SOC_{max}, \forall\, h \quad (8)$$

where SOC_h is the SOC level of the h^{th} EV.

3) Load Modelling

The total load at bu^{th} bus $\big(L(bu,t)\big)$ at any t^{th} time interval is written as follows:

$$L(bu,t) = CL(bu,t) + CSL(bu,t) - SDG(bu,t), \forall\, bu,t \quad (9)$$

where $CSL(bu,t)$ is the load due to PFCS at bus bu, if it is connected to bu^{th} bus, otherwise zero. On the other hand, $SDG(bu,t)$ is the generation from PV at bus bu, if it is connected to bu^{th} bus, otherwise zero.

The load at g^{th} CS at t^{th} time $\big(CSL(g,t)\big)$, which may be connected to any bu^{th} bus, is calculated as follows.

$$CSL(g,t) = \sum_{h=1}^{EV} EVL(g,h,t), \quad \forall\, t \quad (10)$$

where $EVL(g,h,t)$ is the load due to EV_h at g^{th} CS at t^{th} hour when $A^{time}(g,h) < t < D^{time}(g,h)$. $A^{time}(g,h)$ and $D^{time}(g,h)$ are the arrival time and departure time respectively of the EV_h at CS_g.

4) Energy Requirement of EVs

Arrival time, first trip distance and daily mileage are the uncertain variables for all the EV. Arrival SOC, departure SOC and departure time of EV are also uncertain which are calculated based on pre-mentioned uncertainties. Energy requirement by an EV depends on the arrival SOC $(A^{soc}(h))$ and departure SOC $(D^{soc}(h))$ of the h^{th} vehicle. The arrival SOC is related to final first trip distance $(d_{ff}(h))$ in km, whereas departure SOC is associated with subsequent trip distance $(STD(h))$ in km. Energy requirement (kWh) $(R^{eng}(h))$ by h^{th} EV is evaluated as follows (Mehta et al. 2018).

$$R^{eng}(h) = \big(R^{soc}(h) \cdot Bc(h)\big)/\eta_{ch}, \forall\, h, \text{where } Bc \in fn(h) \quad (11)$$

where $R^{soc}(h)$ and $Bc(h)$ indicate required SOC and battery capacity of h^{th} vehicle respectively, η_{ch} is charging efficiency. Req^{soc} is calculated in percentage (Mehta et al. 2018) as follows.

$$R^{soc}(h) = \begin{cases} 1 - A^{soc}(h), & if\ D^{soc}(h) > 1 \\ (D^{soc}(h) - A^{soc}(h), & if\ A^{soc}(h) < (D^{soc}(h) < 1 \\ 0, & if\ A_v^{soc} = (D^{soc}(h) \end{cases} \quad (12)$$

Arrival SOC (Rezaee et al. 2013) and departure SOC (Mehta et al. 2018) are calculated as (13) and (14) respectively.

$$A^{soc}(h) = 1 - \frac{d_{if}(h)}{AER(h)} - \frac{\zeta_c(g,h)}{Bc(h)}, \text{where, } AER \in fn(h) \quad (13)$$

$$D^{soc}(h) = (STD(h)/AER(h)) + 0.25 \quad (14)$$

where $\zeta_c(g,h)$ is consumed energy by h^{th} EV to reach g^{th} PFCS considering traffic congestion, which is calculated as (31) in the second stage. $d_{if}(h)$ is the initial first trip distance, $Bc(h)$ is battery capacity, $AER(h)$ is all-electric range and $STD(h)$ is the subsequent trip distance of h^{th} vehicle which is obtained as (Mehta et al. 2018), by

$$STD(h) = dm(h) - d_{ff}(h) \quad (15)$$

where $d_{ff}(h)$ is the final first trip distance, which is obtained in the second stage as (30). $dm(h)$ is daily mileage of h^{th} vehicle in km. Departure time $(D^{time}(h))$ of h^{th} vehicle is found out using

$$D^{time}(h) = A^{time}(h) + R^{time}(h) \quad (16)$$

where $R^{time}(h)$ is the required time to attain the desire charge level of EV_h, $A^{time}(h)$ is the arrival time of h^{th} vehicle at PFCS. Required time for charging of EV_h with C_r charging rate is calculated as:

$$R^{time}(h) = R^{eng}(h)/C_r \quad (17)$$

5) SDG modelling

The main stochastic variable for PV is solar irradiance (kW/m^2). PV cell temperature is also uncertain but it depends on irradiance only. PV power output at t^{th} hour $\big(Pw_{pv}(t)\big)$ will be added in (9) as a negative load and is expressed as (Sultana and Roy 2015):

$$SDG(t) = Pw_{pv}(t) = Pv_{vari}(t) \times Pw_{pv}, \forall\, t \quad (18)$$

where Pv_{vari} is the 24 hours variation of solar irradiance in p.u. is followed as (Sultana and Roy 2015). Therefore, at the endpoint PV power $\big(Pw_{pv}\big)$ is calculated from solar irradiance (Soroudi et al. 2012) by

$$Pw_{pv} = N_p \cdot F_f \cdot V_{ir} \cdot I_{ir} \quad (19)$$

where N_p is total number of PV module, F_f is the fill factor is presented as:

$$F_f = \frac{V_{mp} \cdot I_{mp}}{V_{oc} \cdot I_{sc}} \quad (20)$$

$$V_{ir} = V_{oc} - C_v \times t_{cell} \quad (21)$$

$$I_{ir} = ir_{avg}\{I_{sc} + C_i(t_{cell} - 25)\} \quad (22)$$

$$t_{cell} = t_{amb} + \big(ir_{avg} \cdot (t_{nom} - 20)/0.8\big) \quad (23)$$

where V_{mp} and I_{mp} are maximum power point voltage and current respectively. V_{oc} and I_{sc} are open circuit voltage and short circuit current. ir_{avg} is average solar irradiance, t_{cell} is the cell temperature in °C. C_v and C_i are voltage and current temperature coefficient. t_{nom} is nominal operating temperature of PV cell. t_{amb} is ambient temperature. The solar irradiance follows beta distribution (Soroudi et al. 2012), which is demonstrated as follows.

$$f(ir) = \begin{cases} \frac{\Gamma(\alpha_{ir} + \beta_{ir})}{\Gamma(\alpha_{ir})\Gamma(\beta_{ir})} \times ir^{(\alpha_{ir}-1)} \times (1-ir)^{(\beta_{ir}-1)}, \\ \qquad if\ 0 \leq ir \leq 1;\ \alpha_{ir} \geq 0;\ \beta_{ir} \geq 0 \\ 0, \quad else \end{cases} \quad (30)$$

where α_{ir} and β_{ir} are beta shape parameters. μ_{ir} and σ_{ir} are the mean and SD of solar irradiance, which is determined as:

$$\mu_{ir} = \alpha_{ir}/(\alpha_{ir} + \beta_{ir}) \quad (24)$$

$$\sigma_{ir} = \sqrt{\mu_{ir}^2(1+\mu_{ir})/(\alpha_{ir}+\mu_{ir})} \quad (25)$$

B. Stage 2: PFCS Selection by EVs

The main goal is to assign each EV to right PFCS by consuming less quantity of energy while reaching its suggested PFCS. This is determined using integer linear programming considering congestions and shortest distances. The shortest paths and distances may be identified using Dijkstra's algorithm (Amaliah et al. 2016). The formulation for optimal section of PFCS by the ILP is discussed below.

1) Assignment Matrix for ILP

The linear programming problem (ILPP) is formulated by an assignment matrix $\psi(g,h)$ (Das et al. 2020) where $h >> g$ and each EV is assigned to a PFCS. This matrix is grounded on the renowned assignment problem (Aktel et al. 2017) with the combination of traffic flow structure (Schrieber et al. 2017). Since, traffic flow is a dynamic event, hence, it is expressed as $\psi(g,h,t)$, where, $t \in time$. The matrix is shown in the Table 1.

TABLE 1
STRUCTURE OF EV ASSIGNMENT MATRIX TO THE PFCS

	EV_1	EV_2	EV_3	...	EV_h
CS_1	$\psi(1,1,t)$	$\psi(1,2,t)$	$\psi(1,3,t)$	...	$\psi(1,h,t)$
CS_2	$\psi(2,1,t)$	$\psi(2,2,t)$	$\psi(2,3,t)$	...	$\psi(2,h,t)$
⋮	⋮	⋮	⋮	⋮	⋮
CS_g	$A(g,1,t)$	$\psi(g,2,t)$	$\psi(g,3,t)$	...	$\psi(g,h,t)$

2) Objective Function-2 (F_2)

In this formulation, the main objective is to keep the battery energy consumption minimum by the EV to reach at PFCS considering traffic congestions at time t, i.e.

$$F_2 = min\left\{\sum_{g=1}^{CS}\sum_{h=1}^{EV}(\zeta_c(g,h,t)\cdot\chi(g,h,t))\right\} \quad (26)$$

$$\chi(g,h,t) = \begin{cases}1, & \text{if } EV_h \text{ is assigned to } CS_g \text{ at time } t\\ 0, & \text{otherwise}\end{cases} \quad (27)$$

3) Constraints

$$\sum_{g=1}^{cs}\chi(g,h,t) = 1, \forall\, EV_h \quad (28)$$

$$(g,h) \le d_{ff}(h) \quad (29)$$

$$d_{ff}(h) \in d_{if}(h) \cup \mathbb{d}(g,h) \quad (30)$$

where in (28), $1 \le h \le EV$ and each EV is assigned to only one PFCS at a time. In (29), the final first trip distance should not be the lower than the distance of EV_h from CS_g charging stations $\mathbb{d}(g,h)$.

4) Energy modelling of EVs

In order to model the energy consumption by the EV considering traffic congestions and distance, various factors such as the distance between the location of the vehicle and the charging station, vehicles speed considering congestion $(\mathcal{v}_m(g,h,t))$, all electric range (AER) of the individual vehicles, battery capacity of the EV, vehicles flow $(y(g,h,t))$ and jam coefficient $\left(\mathbb{C}_j(g,h)\right)$ are considered [25]. The consumed energy by EV_h considering the vehicles flow and traffic congestions it is written as (Mkahl 2015):

$$\zeta_c(g,h) = \frac{Bc(h)\cdot\tau(g,h,t)\cdot\ \mathcal{v}_m(g,h,t)}{AER\cdot\mathbb{C}_j(g,h)} \quad (31)$$

Again, from the equation of Greenshields model (Shlayan et al. 2018), the modified velocity of the EV due to traffic congestion is presented as:

$$\mathcal{v}_m(g,h,t) = v_f(g,h)\left(1 - y(g,h,t)\cdot\tau(g,h,t)\cdot\mathbb{C}_j(g,h)\ /\ \mathbb{d}(g,h)\right) \quad (32)$$

where $v_f(g,h)$ is the free flow velocity and the required time $\tau(g,h,t)$ for covering the distance $\left(\mathbb{d}(g,h)\right)$ with vehicle flow $y(g,h,t)$ by the EV is expressed as (Mkahl et al. 2017):

$$\tau(g,h,t) = v_f\ (g,h)/2\cdot\frac{v_f(g,h)\cdot y(g,h,t)}{\mathbb{C}_j(g,h)\cdot d(g,h)} \quad (33)$$

III. SOLUTION METHODOLOGY

The HHO technique, 2m PEM and the algorithm for this proposed work, are presented below.

A. Harris Hawks Optimization (HHO)

In 2019, A.A. Heidari et al. introduced the HHO (Heidari et al. 2019). This optimization is based on chasing tactic of Harris' hawks to its target. The key steps are instructed as follows (Heidari et al. 2019).

1) Initialization

Decision variables (K_{ij}), preliminary energy (En_0) and jump strength (Js) are initialized as follows.

$$K_{ij} = K_j^{min} + rand\left(K_j^{max} - K_j^{min}\right), where\ i = 1,2,3\ldots S_p;\ j = 1,2,3\ldots D_n \quad (34)$$

$$En_0 = 2\cdot rand(-1,1) - 1 \quad (35)$$

$$Js = 2\left(1 - rand(0,1)\right) \quad (36)$$

2) Update part

The energy (En) is updated in every iteration (t) as:

$$En = 2\cdot En_0\left(1 - \frac{t}{T}\right) \quad (37)$$

where number of iteration is T. Decision vector $\left(K^{(Z+1)}\right)$ is updated according to various situations as follows.

- *Exploration phase (if $|En| \ge 1$)*

$$K^{(Z+1)} = \begin{cases} K_{rand}^{(Z)} - m_1\left|K_{rand}^{(Z)} - 2m_2K^{(Z)}\right|, & if\ q \ge 0.5\\ K_{rabbit}^{(Z)} - K_m^{(Z)} - m_3\left(LL + m_4(UL - LL)\right), & if\ q < 0\end{cases} \quad (38)$$

where Z is iteration number, $K_{rabbit}^{(Z)}$ is the position of the rabbit. $K_{rand}^{(Z)}$ is randomly selected hawk position. m_1, m_2, m_3, m_4 and q is random number $\in [0,\ 1]$. UL is upper limit and LL is lower limit of the decision variables.

- *Exploitation phase* $(if\ |En| < 1)$

The different conditions in this phase as follows, where r is the possibility of a rabbit can run away.

- Soft besiege $(if\ r \ge 0.5\ and\ |En| \ge 0.5)$

$$K^{(Z+1)} = \Delta K^{(Z)} - E\left|Js\cdot K_{rabbit}^{(Z)} - K^{(Z)}\right| \quad (39)$$

- Hard besiege $(if\ r \ge 0.5\ and\ |En| < 0.5)$

$$K^{(Z+1)} = K_{rabbit}^{(Z)} - E\left|\Delta K^{(Z)}\right| \quad (40)$$

- Soft besiege with progressive rapid dives $(if\ r < 0.5\ and\ |En| \ge 0.5)$

$$K^{(Z+1)} = \begin{cases}A, & if\ F(A) < F\left(K^{(Z)}\right)\\ B, & if\ F(B) < F\left(K^{(Z)}\right)\end{cases} \quad (41)$$

- Hard besiege with progressive rapid dives ($if\ r < 0.5\ and\ |En| < 0.5$)

$$K^{(Z+1)} = \begin{cases} X, & if\ F(A) < F\left(K^{(Z)}\right) \\ Y, & if\ F(B) < F\left(K^{(Z)}\right) \end{cases} \quad (42)$$

Detail information about the variables used in above steps are available in (Heidari et al. 2019).

B. Hong's 2m-Point estimation Method

Hong's 2m PEM (Hong 1998) is applied in this work which is an effective statistical technique to handle multiple uncertainties. The objective functions (F_1, F_2) are modified to mean values $(\mu F_1, \mu F_2)$ according to 2m PEM as follows.

$$Min(F) = Min(\mu F), where\ F \in F_1\ or\ F_2 \quad (43)$$

$$\mu F = F(1) \quad (44)$$

Standard deviation (SD) of objective function is calculated by

$$\sigma F = \sqrt{(F(2) - (F(1))^2)} \quad (45)$$

where $F(1)$ is the first moment and $F(2)$ is the and second moment of the objective function (F), which are obtained as follows.

$$F(h) = \sum_{l=1}^{m} \sum_{po=1}^{2} \left(w_{l,po} \left(F_{l,po} \right)^h \right),\ h \in 1,2 \quad (46)$$

$$w_{l,po} = \frac{(-1)^{po}}{m} \cdot \frac{\xi_{R_l,(3-po)}}{\xi_{R_l,1} - \xi_{R_l,2}},\ po \in 1,2 \quad (47)$$

$$F_{l,po} = f\left(D_v, \mu_{R_1}, \mu_{R_2}, \dots, z_{l,po}, \dots, \mu_{R_m}\right), \quad po \in 1,2;\ l \in 1,2,3,\dots,m \quad (48)$$

where $F(h)$ is the h^{th} moment of F. $po \in 1,2$ generate two weighting factors $(w_{l,po})$ of z_l. m represents the number of uncertain variable. ξ_{R_l} is the standard location of R_l. D_v is deterministic variable, μ_{R_l} is the mean of the l^{th} uncertain variable. $z_{l,po}$ is definite positions of the input variable.

$2 \times m$ number of sets are created using (48). The objective functions F_1 and F_2 are calculated for all stochastic set clubbed with a fixed deterministic set. In this present work, the sizes of the SDG and locations of the PFCS and SDG are the deterministic variables (D). The PEM sets are expressed as:

$$f\left(D_v, \mu_{R_1}, \mu_{R_2}, \dots, z_{l,po}, \dots, \mu_{R_m}\right) = \underbrace{\begin{bmatrix} D_1 & D_2 & \dots & D_n \\ D_1 & D_2 & \dots & D_n \\ D_1 & D_2 & \dots & D_n \\ D_1 & D_2 & \dots & D_n \\ \vdots & \vdots & \vdots & \vdots \\ D_1 & D_2 & \dots & D_n \\ D_1 & D_2 & \dots & D_n \end{bmatrix}}_{Deterministics\ Part} \underbrace{\begin{bmatrix} z_{1,1} & \mu_{R_2} & \mu_{R_3} & \dots & \mu_{R_m} \\ z_{1,1} & \mu_{R_2} & \mu_{R_2} & \dots & \mu_{R_m} \\ \mu_{R_1} & z_{2,1} & \mu_{R_3} & \dots & \mu_{R_m} \\ \mu_{R_1} & z_{2,2} & \mu_{R_3} & \dots & \mu_{R_m} \\ \vdots & \vdots & \vdots & \vdots & \vdots \\ \mu_{R_1} & \mu_{R_2} & \mu_{R_3} & \dots & z_{m,1} \\ \mu_{R_1} & \mu_{R_2} & \mu_{R_3} & \dots & z_{m,2} \end{bmatrix}}_{Stochastic\ Part} \quad (49)$$

where n is the number of deterministic variable.

$$z_{l,po} = \mu_{R_l} + \left(\xi_{R_l,po} \times \sigma_{R_l}\right), \quad po = 1,2 \quad (50)$$

where σ_{R_l} is the standard deviation of the uncertain variable.

$$\xi_{R_l,po} = \frac{\lambda_{R_l,3}}{2} + (-1)^{3-po} \sqrt{\lambda_{R_l,4} - 3\lambda_{R_l,3}^2/4}, \quad po \in 1,2 \quad (51)$$

where $\xi_{R_l,po}$ is the po^{th} standard location of R_l. $\lambda_{R_l,3}$ and $\lambda_{R_l,4}$ are the coefficient of third central moment//skewness and coefficient of fourth central moment/kurtosis of R_l respectively.

$$\lambda_{R_l,k} = \mathbb{E}\left[\left(R_l - \mu_{R_l}\right)^k\right] / \left(\sigma_{R_l}\right)^k, \quad k \in 3,4 \quad (52)$$

where $\mathbb{E}$ is the notation for expected value and $\mathbb{E}\left[\left(R_l - \mu_{R_l}\right)^k\right]$ is calculated using

$$\mathbb{E}\left[\left(R_l - \mu_{R_l}\right)^k\right] = \sum_{j=1}^{NO} \left(R_{l,j} - \mu_{R_l}\right)^k \cdot \mathbb{P}\left(R_{l,j}\right), \quad k \in 3,4 \quad (53)$$

where $R_{l,j}$ is the value produced from distribution function at j^{th} observation, NO is the number of inspection of R_l. $\mathbb{P}\left(R_{l,j}\right)$ signifies the probability density of $R_{l,j}$. R_l is generated by (54) for normal distribution.

$$R_l = \mu_{uv} + (\mathbb{z} \times \sigma_{uv}), \quad l \in 1,2,3,\dots,m \quad (54)$$

where μ_{uv} and σ_{uv} is the mean and SD of the uncertain variable uv respectively, $\mathbb{z}$ is the standard normal random value. The probability density of R_l is obtainable by

$$\mathbb{P}(R_l) = \left(e^{-\left[\left(R_l - \mu_{R_l}\right)^2 / 2\left(\sigma_{R_l}\right)^2\right]} \right) / \sqrt{2\pi {\sigma_{R_l}}^2} \quad (55)$$

C. Algorithm of Proposed Work

Start

Initialization

1. Initialize the decision variables (PFCS locations, SDG locations, SDG sizes).

Objective Function Calculation

Under 2m PEM

2. Set time interval, $t = 0$.
3. Find out the shortest path and distance to the PFCSs from the EVs at t^{th} time interval using Dijkstra's algorithm
4. Find out the energy consumption by the EVs to reach PFCSs considering congestions using (31).
5. Assign the EVs to apt PFCS by consuming the least energy using ILP.
6. Calculate the final energy requirement by the EVs using (11).
7. Calculate the total load for every PFCS at t^{th} time interval.
8. Find the SDG generations at t^{th} time interval.
9. Run the backward forward sweep load for to calculate power loss at t^{th} time interval.
10. $t = t + 1$.
11. Go to next step if $t = T$, otherwise go to step 3.
12. Calculate the energy loss.
13. Calculate the mean and SD of the objective function

Update

14. Update the decision variables using optimization techniques.
15. Go to next step if optimization is converged, otherwise go to step 2.
16. Display the optimized results.

end

IV. Simulation Study

A. Input Data

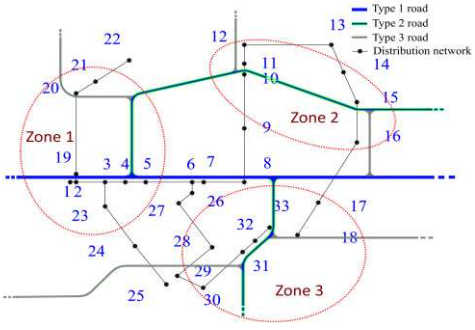

Fig. 1. Superimposed study area with power distribution and traffic network.

Figure 1 shows the area, where a 33 node distribution network (Amiri et al. 2018) is overlapped with a traffic

network. Zone wise allocation of PFCS is necessary for well accessibility of charging station to all EV users in a city. Therefore, three zones are identified based on the vehicle density caused by market place, housing area, land accessibility and road arrangement.

Three different types of roads are taken here, where the busiest road is type 1, next to it is the type 2 and the least busy roads are type 3. Based on one year's vehicle behaviours, it is observed that the peak vehicle flow varies 500-1000 vehicle/hr for different sections of the roads and figure 2 shows the hourly profile of vehicle flow of the three types of road. Table 2 present the jam coefficients (Mkahl et al. 2017) for different types of the road.

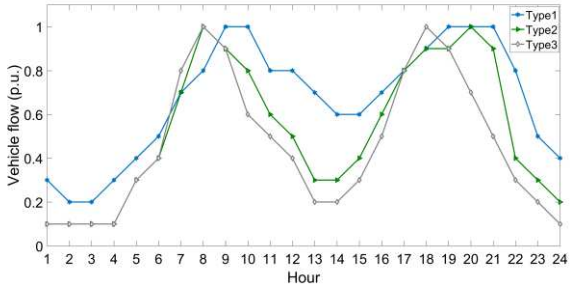

Fig. 2. Annual average vehicle flow profile of three types of road.

TABLE 2
ELECTRIC VEHICLE TYPES AND SPECIFICATION

	Road Type 1	Road Type 2	Road Type 3
Jam Coefficient	250	200	150

The distribution, mean value, standard deviation and maximum, minimum values of different variables associated with EVs are presented in Table 3 and the uncertain data related to solar PV are taken as (Soroudi et al. 2012). Annual average PV profile and conventional load profile are shown in Figure 3 as (Pal et al. 2020).

TABLE 3
DISTRIBUTION DETAILS FOR UNCERTAIN PROPERTIES OF EV

Variable	Unit	Distribution	Mean	Std. dev.	Min	Max
Arrival time	hour	Truncated Gaussian (Shafie-khah et al. 2016)	12	5	4	24
Daily mileage	km	Normal (Mehta et al. 2018)	55	10	0	-
First trip distance	km	Normal (Mehta et al. 2018)	19.25	7.95	0	-

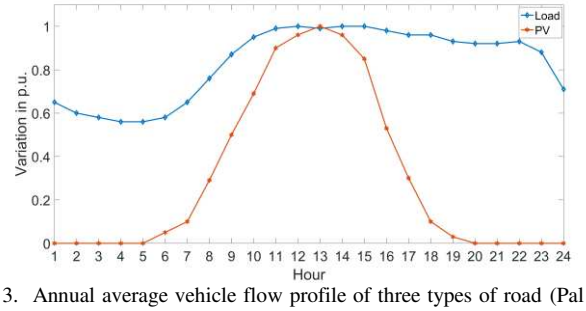

Fig. 3. Annual average vehicle flow profile of three types of road (Pal et al. 2020).

In this work, level 2 (fast) charging facility is considered with 22 kW (Awasthi et al. 2017; Collin et al. 2019; Andrade et al. 2020). Charging efficiency is considered 95% (Mohamed et al. 2014; Bodo et al. 2017). The arrival SOC is limited to 25 – 90% (Shafie-khah et al. 2016; Pal et al. 2021).

TABLE 4
ELECTRIC VEHICLE TYPES AND SPECIFICATIONS (MEHTA ET AL. 2018)

Type of EV	Battery Capacity (kWh)	AER (km)	Presence (%) in the Area
T1	13.8	48.27	60
T2	18.4	64.36	30
T3	24	117	10

Different types of vehicle are present in a city with different battery capacities. Hence, three types of EV are taken in this work and shown in Table 4. Total 200 EVs are considered in the proposed study area.

B. Simulation Case Study

In this work, the simulations are performed in MATLAB coding platform in a computer with Intel Core i5, 8 GB ram. Three case studies are conducted to check the performances of the proposed allocation strategy considering the uncertainties by 2m PEM. The case studies are defined as follows:

1) Case-1: In this study, the PFCSs are allocated without the presence of SDG and the EVs are not assigned at apt PFCSs using ILP, rather it is coming to CS whichever is nearest by Dijkstra's algorithm.

2) Case-2: This case is also for PFCS allocation without SDG but EVs are assigned at proper PFCSs considering the traffic congestions and distances by ILP and Dijkstra's algorithm.

3) Case-3: In this study, the optimized sizes and locations of SDG are achieved along with PFCS locations, where apt choice of PFCSs by the EVs is also taken into account.

Table 5 and Table 6 present the solutions for the case-1 and case-2 respectively for 100% EV penetration, where the optimal locations of PFCS using GWO and HHO are shown with minimized means of the energy loss and obtained standard deviations.

TABLE 5
ALLOCATED LOCATIONS OF PFCS AND ENERGY LOSS FOR CASE-1 WITH 100% EV PENETRATION

Optimization Technique	PFCS Location (Node)			Mean Energy Loss (kWh)	SD Energy loss (kWh)
GWO	2	10	28	4940.9903	26.5687
HHO	2	10	28	4940.9903	26.5687

TABLE 6
ALLOCATED LOCATIONS OF PFCS AND ENERGY LOSS FOR CASE-2 WITH 100% EV PENETRATION

Optimization Technique	PFCS Location (Node)			Mean Energy Loss (kWh)	SD Energy loss (kWh)
GWO	2	16	28	4336.6315	24.3021
HHO	2	16	28	4336.6315	24.3021

In table 5, the optimal locations of PFCS for case-1 are 2, 10 and 28, and Table 6 shows the locations are 2, 16 and 28 for case-2. It is observed from Table 5 and Table 6 that one PFCS's location is changed from node 10 to 16 in case-2 and the energy loss is reduced compared to case-1. In case-1, the locations are closest to the substation in each zone to keep the system loss minimum. As, in this case, the EVs are assigned to nearest PFCS only and their energy loss due to travel was not the concern. Therefore, the PFCS locations are only motivated to reduce the power system energy loss, not the energy demand by

the EVs. However, in case-2, the energy requirement by the EVs to travel up to PFCSs are also taken care, which helps to reduce the SOC requirement of the EVs. Hence, for the locations of node 2, 16 and 28, the energy loss is less due to less energy demand by the EVs compared to case-1.

The allocation results of PFCSs and SDGs are shown in Table 7 with 100% EV penetration. In this case, HHO obtains less energy loss by allocating SDG at proper locations with apt sizes w.r.t. GWO. It is seen from Table 6 and Table 7 that one location of PFCS is changed from node 28 to 31 in case-3 for the simultaneous allocation of PFCSs and SDGs. Significant energy loss reduction is achieved in case-3 due to the optimal presence of SDGs.

TABLE 7
LOCATIONS OF PFCS AND LOCATIONS WITH SIZES OF SDG FOR CASE-3 WITH 100% EV PENETRATION

Optimization Technique	GWO			HHO		
PFCS Location (Node)	2	16	31	2	16	31
SDG Location (Node)	3	14	30	24	14	30
SDG size (MW)	2.2354	1.1075	1.3128	1.4046	1.1417	1.3904
Mean Energy Loss (kWh)	2961.0982			2918.5838		
SD Energy loss (kWh)	28.4861			28.8568		

Again it is noticed from Table 5-7, that both the optimization techniques provide the same solution for case-1 as well as for case-2. But in case-3, HHO performs better than GWO. Figure 4 depicts the convergence curves for all the cases with 100% EV penetration. It is observed in Figure 4 that the HHO converged before the GWO. Moreover, HHO provides better loss minimization in case-3 compared to GWO.

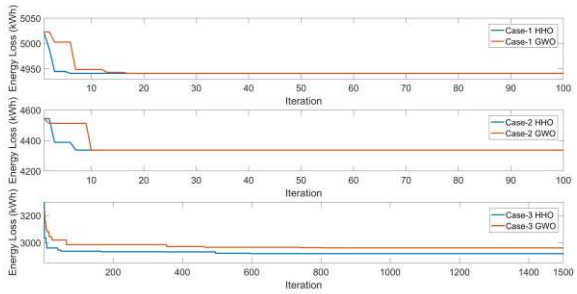

Fig. 4. Convergence curves of GWO and HHO for case-1 to 3 with 100% EV penetration.

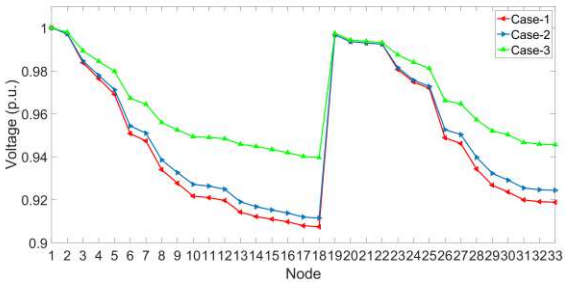

Fig. 5. Daily average voltage profiles of the distribution network for case-1 to 3 with 100% EV penetration.

Figure 5 illustrates the daily average voltage profiles of the distribution network for all the cases with 100% EV penetration. It is seen in Figure 5, the voltage profile is worst among all for case-1, because of the allocation of PFCSs with mismanagement of EVs appointment to the PFCSs. The voltage profile of case-2 is comparatively better than case-1, which is the allocation of PFCSs at apt locations considering proper assigned EVs to the PFCSs by ILP. For case-3, the voltage profile is far improved due to the allocations of SDGs.

C. *Sensitivity Analysis*

The same three cases are performed with 50% EV penetration and Table 8 shows the respective results. It shows that the locations of the PFCS and SDG with 50% EV penetration are same as locations in case of 100% EV penetration for all the three cases, which confirm the robustness of the solutions. Also, both the optimization techniques are reached to the same solutions for all the cases with 50% EV penetration scenario. Like 100% EV penetration, the energy loss is more for case-1, and reduced in case-2. Case-3 offers the best among all with least energy loss. However, the energy losses are less compared to 100% EV penetration.

TABLE 8
SOLUTIONS FOR CASE-1 TO CASE-3 WITH 50% EV PENETRATION

	Optimization Technique	GWO			HHO		
Case-1	PFCS Location (Node)	2	10	28	2	10	28
	Mean Energy Loss (kWh)	4573.6032			4573.6032		
	SD Energy loss (kWh)	18.2569			18.2569		
Case-2	PFCS Location (Node)	2	16	28	2	16	28
	Mean Energy Loss (kWh)	4190.3649			4190.3649		
	SD Energy loss (kWh)	17.0458			17. 0458		
Case-3	PFCS Location (Node)	2	16	31	2	16	31
	SDG Location (Node)	24	14	30	24	14	30
	SDG size (MW)	1.396	1.054	1.371	1.396	1.054	1.371
	Mean Energy Loss (kWh)	2894.4277			2894.4277		
	SD Energy loss (kWh)	25.4753			25.4753		

Figure 6 shows the energy loss comparisons between 100% and 50% EV penetration and it is visualized that the energy losses are less for all cases in 50% EV penetration scenario compare to 100% penetration because of less number of EV creates comparatively less load and less energy demand in the system. Energy losses are also decreasing from case-1 towards case-3 for both the EV penetration level due to case wise development, i.e. apt assignment of EV at PFCSs and allocation of SDGs at proper nodes with suitable sizes.

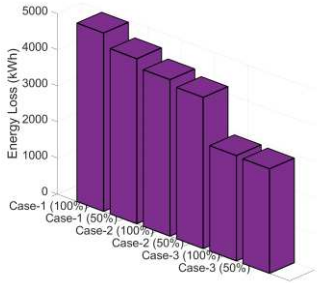

Fig. 6. Comparison of all the cases with 100% and 50% EV penetration.

Table 9 presents the sensitivity studies on different key items. It is noticed, when SDGs sizes are reduced (study-2), the energy loss is increased significantly. High EV penetration (study-3) and low charging efficiency (study-4) both create extra load on the power system, which leads to increment of energy loss. The energy loss is not affected by the increment of 20% traffic flow (study-5), whereas 50% increment increases energy loss (study-6), because traffic flow creates congestions which burn more energy of the EV batteries and increase the energy demand from

the system. Increased jam coefficient defines, the jam will be occurred with more number of vehicle. Therefore, increased jam coefficient reduces the congestions and consequently energy loss is also reduced (study-7).

TABLE 9
SENSITIVITY ANALYSIS ON THE KEY FACTORS FOR CASE-3

Study	Test Item	Mean Energy Loss (kWh)	Change from study-1 (%)
1	Base Case-3 with 100% EV and 100% DG	2918.5838	-
2	Decrease SDG sizes by 50%	3254.1446	▲11.49
3	Increase EV penetration to 120%	2958.3145	▲1.36
4	Decrease charging efficiency to 80%	2921.1453	▲0.08
5	Increase traffic flow by 20%	2918.5838	▲0
6	Increase traffic flow by 50%	2922.4563	▲0.13
7	Increase jam coefficient by 20%	2917.1569	▼0.04

▲ – Increased, ▼ – Decreased

Figure 7 depicts the daily average voltage profiles of the different sensitivity studies. It is seen in case of voltage also, reduction of SDG's sizes (study-2) drops the voltage profile remarkably. Voltage profiles are not significantly deviated from the base case (study-1) in case of study-3 & 4. Whereas, voltage profile is not affected in study 5 – 7 and it is same as study-1.

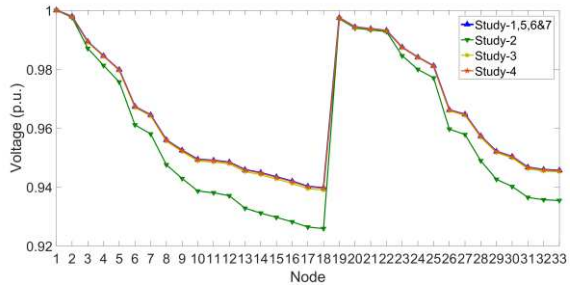

Fig. 7. Daily average voltage profiles of different sensitivity studies.

D. Validation of the Solution

The actual targeted problem of this proposed work which is case-3 with 100% EV penetration, is solved with eight other optimization techniques and the solutions are presented in Table 10. The selected optimization techniques are Honey Bee Colony (HBC), Backtracking Search Optimization Algorithm (BSA), Differential Evolution (DE), Biogeography Based Optimization (BBO), Symbiotic Organisms Search (SOS), Genetic Algorithm (GA), Particle Swarm Optimization (PSO) and Henry Gas Solubility Optimization (HGSO).

TABLE 10
SOLUTIONS OF CASE-3 WITH DIFFERENT OPTIMIZATION TECHNIQUES FOR 100% EV PENETRATION

Optimization Technique	PFCS Locations			SDG Location and Size (MW)			Mean Energy Loss (kWh)	SD Energy Loss (kWh)
HBC	2	16	31	6	15	31	2968.1383	30.2487
				1.561	0.941	0.905		
BSA	2	16	31	3	14	30	2961.0982	29.1257
				2.235	1.107	1.312		
DE	2	16	31	3	14	30	2961.0982	29.1257
				2.236	1.106	1.313		
BBO	2	16	31	3	14	30	2961.0982	29.1257
				2.235	1.107	1.313		
SOS	2	16	31	3	14	30	2961.0982	29.1257
				2.235	1.107	1.312		
GA	2	16	31	3	14	30	2961.0981	29.1257
				2.236	1.107	1.312		
PSO	2	16	31	24	14	30	2918.5838	28.8568
				1.404	1.141	1.390		
HGSO	2	16	31	24	14	30	2918.5838	28.8568
				1.404	1.141	1.390		
GWO	2	16	31	3	14	30	2961.0982	28.4861
				2.235	1.107	1.312		
HHO	2	16	31	24	14	30	2918.5838	28.8568
				1.404	1.141	1.390		

In Table 10, the solution given by HBC is the lowest loss minimization among all, whereas PSO and HGSO perform same as HHO and minimized the remarkable energy loss compared to other techniques. Therefore, it can be decided that the location 2, 16 and 31 for PFCS and 24, 14 and 30 for SDGs with sizes 1.4, 1.1 and 1.3 MW respectively, are the optimized solution to achieve minimum energy loss for the proposed problem.

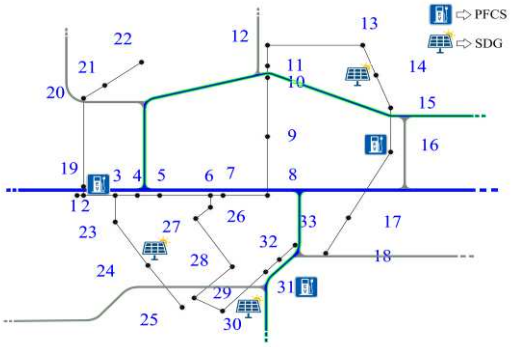

Fig. 8. Allocation of PFCSs and SDGs.

Figure 8 shows the graphical allocation of PFCSs and SDGs, where it is easily noticeable that the PFCSs are scattered in the area which will offer well accessibility to all EV users with less travel distance.

E. Statistical Hypothesis Test

The statistical tests, wilcoxon signed rank test (Liu et al. 2017) and quade test (Liu et al. 2017) are performed to check robustness of the solutions of the targeted problem and to confirm the hypothesis. Both the test are performed for 30 sample with 95% confidence interval. The absolute values are 137 (from alpha distribution table) for wilcoxon signed rank test and 2.73 (from f distribution table) for quade test.

1) Wilcoxon Signed Rank Test

The wilcoxon signed rank test is executed with 95% confidence considering 30 samples and the results are shown in Table 11. It is seen that the test values are higher than the absolute value (137), for every optimization technique, which accept the null hypothesis (H_0) and confirm the constancy and robustness of the results.

TABLE 11
WILCOXON TEST RESULT

	HBC	BSA	DE	BBO	SOS	GA	PSO	HGSO	GWO	HHO
Test Value	191	182	198	185	171	208	196	183	202	210
H_0?	✓	✓	✓	✓	✓	✓	✓	✓	✓	✓

2) Quade Test

Quade Test is performed with same confidence interval and same sample size. Table 12 presents the test value considering 10 optimization techniques. H_0 is rejected here for the higher statistic value than the absolute value (2.73), which confirms significant better performance of HHO, PSO and HGSO.

TABLE 12
QUADE TEST RESULT

No. of Scenario	No. Optimization Technique	Alpha	Test Value	H_0?
30	10	0.05	55.83	✗

V. CONCLUSION

Lack of public charging station is the key obstacle for large scale acceptance of EVs. This article proposed a realistic solution for PFCS placement in a distribution network considering the traffic network. The locations are found out where the energy loss is minimum. The SDGs are also allocated for further reduction of energy loss and to improve the voltages. The EVs are assigned at apt PFCSs by ILP with Dijkstra's algorithm considering traffic congestions and shortest distances. The apt assignment of EVs reduces the energy loss indirectly. The locations and sizes of SDG are as important as PFCS locations in terms of energy loss minimization. Total 10 optimization techniques are used to validate the final allocation result. The statistical tests show the sturdiness of the result. For the future work, battery energy storages can be connected to schedule the power generated from SDGs. The required expansion of the network can also be planned.

DECLARATIONS

Funding: There is no funding for this work.

Conflicts of interest/Competing interests: The authors declare that they have no conflict of interest.

Availability of data and material: Data are available with the authors.

Code availability: Codes are available with the authors.

Authors' contributions: Arnab Pal: Conceptualization, Methodology, Software, Writing-original draft. **Aniruddha Bhattacharya:** Conceptualization, Methodology, Supervision, Writing-review & editing. **Ajoy Kumar Chakraborty:** Conceptualization, Methodology, Supervision, Writing-review & editing.

REFERENCES

Aktel A, Yagmahan B, Özcan T, et al (2017) The comparison of the metaheuristic algorithms performances on airport gate assignment problem. Transportation Research Procedia 22:469–478. https://doi.org/10.1016/j.trpro.2017.03.061

Amaliah B, Fatichah C, Riptianingdyah O (2016) FINDING THE SHORTEST PATHS AMONG CITIES IN JAVA ISLAND USING NODE COMBINATION BASED ON DIJKSTRA ALGORITHM. International Journal on Smart Sensing and Intelligent Systems 9:2219–2236. https://doi.org/10.21307/ijssis-2017-961

Amiri SS, Jadid S, Saboori H (2018) Multi-objective optimum charging management of electric vehicles through battery swapping stations. Energy 165:549–562. https://doi.org/10.1016/j.energy.2018.09.167

Andrade J, Ochoa LF, Freitas W (2020) Regional-scale allocation of fast charging stations: travel times and distribution system reinforcements. IET Generation, Transmission & Distribution 14:4225–4233. https://doi.org/10.1049/iet-gtd.2019.1786

Atat R, Ismail M, Serpedin E, Overbye T (2020) Dynamic Joint Allocation of EV Charging Stations and DGs in Spatio-Temporal Expanding Grids. IEEE Access 8:7280–7294. https://doi.org/10.1109/ACCESS.2019.2963860

Awasthi A, Venkitusamy K, Padmanaban S, et al (2017) Optimal planning of electric vehicle charging station at the distribution system using hybrid optimization algorithm. Energy 133:70–78. https://doi.org/10.1016/j.energy.2017.05.094

Bodo N, Levi E, Subotic I, et al (2017) Efficiency Evaluation of Fully Integrated On-Board EV Battery Chargers With Nine-Phase Machines. IEEE Trans Energy Convers 32:257–266. https://doi.org/10.1109/TEC.2016.2606657

Collin R, Miao Y, Yokochi A, et al (2019) Advanced Electric Vehicle Fast-Charging Technologies. Energies 12:1839. https://doi.org/10.3390/en12101839

Das S, Acharjee P, Bhattacharya A (2020) Charging Scheduling of Electric Vehicle incorporating Grid-to-Vehicle (G2V) and Vehicle-to-Grid (V2G) technology considering in Smart-Grid. IEEE Transactions on Industry Applications. https://doi.org/10.1109/TIA.2020.3041808

Davidov S, Pantoš M (2019) Optimization model for charging infrastructure planning with electric power system reliability check. Energy 166:886–894. https://doi.org/10.1016/j.energy.2018.10.150

Dong G, Ma J, Wei R, Haycox J (2019) Electric vehicle charging point placement optimisation by exploiting spatial statistics and maximal coverage location models. Transportation Research Part D: Transport and Environment 67:77–88. https://doi.org/10.1016/j.trd.2018.11.005

Gong D, Tang M, Buchmeister B, Zhang H (2019) Solving Location Problem for Electric Vehicle Charging Stations—A Sharing Charging Model. IEEE Access 7:138391–138402. https://doi.org/10.1109/ACCESS.2019.2943079

Hadian E, Akbari H, Farzinfar M, Saeed S (2020) Optimal Allocation of Electric Vehicle Charging Stations With Adopted Smart Charging/Discharging Schedule. IEEE Access 8:196908–196919. https://doi.org/10.1109/ACCESS.2020.3033662

Heidari AA, Mirjalili S, Faris H, et al (2019) Harris hawks optimization: Algorithm and applications. Future Generation Computer Systems 97:849–872. https://doi.org/10.1016/j.future.2019.02.028

Hong HP (1998) An efficient point estimate method for probabilistic analysis. Reliability Engineering & System Safety 59:261–267. https://doi.org/10.1016/S0951-8320(97)00071-9

Hosseini S, Sarder M (2019) Development of a Bayesian network model for optimal site selection of electric vehicle charging station. International Journal of Electrical Power & Energy Systems 105:110–122. https://doi.org/10.1016/j.ijepes.2018.08.011

Kong W, Luo Y, Feng G, et al (2019) Optimal location planning method of fast charging station for electric vehicles considering operators, drivers, vehicles, traffic flow and power grid. Energy 186:115826. https://doi.org/10.1016/j.energy.2019.07.156

Liu L, Zhang Y, Da C, et al (2020) Optimal allocation of distributed generation and electric vehicle charging stations based on intelligent algorithm and bi-level programming. Int Trans Electr Energ Syst. https://doi.org/10.1002/2050-7038.12366

Liu X, Bie Z (2019) Optimal Allocation Planning for Public EV Charging Station Considering AC and DC Integrated Chargers. Energy Procedia 159:382–387. https://doi.org/10.1016/j.egypro.2018.12.072

Liu Z, Blasch E, John V (2017) Statistical comparison of image fusion algorithms: Recommendations. Information Fusion 36:251–260. https://doi.org/10.1016/j.inffus.2016.12.007

Liu Z, Wen F, Ledwich G (2013) Optimal Planning of Electric-Vehicle Charging Stations in Distribution Systems. IEEE Trans Power Delivery 28:102–110. https://doi.org/10.1109/TPWRD.2012.2223489

Long Y, Xu D, Li X (2019) Channel coordination of battery supplier and battery swap station of micro-grid with uncertain rental demand. Soft Comput 23:9733–9745. https://doi.org/10.1007/s00500-018-3542-x

Luo L, Wu Z, Gu W, et al (2020) Coordinated allocation of distributed generation resources and electric vehicle charging stations in distribution systems with vehicle-to-grid interaction. Energy 192:116631. https://doi.org/10.1016/j.energy.2019.116631

Mehta R, Srinivasan D, Khambadkone AM, et al (2018) Smart Charging Strategies for Optimal Integration of Plug-In Electric Vehicles Within Existing Distribution System Infrastructure. IEEE Trans Smart Grid 9:299–312. https://doi.org/10.1109/TSG.2016.2550559

Mkahl R (2015) Contribution to the modeling, dimensioning and management of the energy flows of an electric vehicle charging system: study of the interconnection with the electric network. Ph.D.dissertation, Univ.Belfort-Montbéliard

Mkahl R, Nait-Sidi-Moh A, Gaber J, Wack M (2017) An optimal solution for charging management of electric vehicles fleets. Electric Power

Systems Research 146:177–188. https://doi.org/10.1016/j.epsr.2016.11.008

Mohamed A, Salehi V, Ma T, Mohammed O (2014) Real-Time Energy Management Algorithm for Plug-In Hybrid Electric Vehicle Charging Parks Involving Sustainable Energy. IEEE Trans Sustain Energy 5:577–586. https://doi.org/10.1109/TSTE.2013.2278544

Motoaki Y (2019) Location-Allocation of Electric Vehicle Fast Chargers—Research and Practice. WEVJ 10:12. https://doi.org/10.3390/wevj10010012

Pal A, Bhattacharya A, Chakraborty AK (2019) Allocation of EV Fast Charging Station with V2G Facility in Distribution Network. In: 2019 8th International Conference on Power Systems (ICPS). IEEE, Jaipur, India, pp 1–6

Pal A, Bhattacharya A, Chakraborty AK (2021) Allocation of electric vehicle charging station considering uncertainties. Sustainable Energy, Grids and Networks 25:100422. https://doi.org/10.1016/j.segan.2020.100422

Pal A, Chakraborty AK, Bhowmik AR (2020) Optimal Placement and Sizing of DG considering Power and Energy Loss Minimization in Distribution System. ijeei 12:624–653. https://doi.org/10.15676/ijeei.2020.12.3.12

Ponnam VKB, Swarnasri K (2020) Multi-Objective Optimal Allocation of Electric Vehicle Charging Stations and Distributed Generators in Radial Distribution Systems using Metaheuristic Optimization Algorithms. Eng Technol Appl Sci Res 10:5837–5844. https://doi.org/10.48084/etasr.3517

Rezaee S, Farjah E, Khorramdel B (2013) Probabilistic Analysis of Plug-In Electric Vehicles Impact on Electrical Grid Through Homes and Parking Lots. IEEE Trans Sustain Energy 4:1024–1033. https://doi.org/10.1109/TSTE.2013.2264498

Sadeghi-Barzani P, Rajabi-Ghahnavieh A, Kazemi-Karegar H (2014) Optimal fast charging station placing and sizing. Applied Energy 125:289–299. https://doi.org/10.1016/j.apenergy.2014.03.077

Schrieber J, Schuhmacher D, Gottschlich C (2017) DOTmark – A Benchmark for Discrete Optimal Transport. IEEE Access 5:271–282. https://doi.org/10.1109/ACCESS.2016.2639065

Shaaban MF, Mohamed S, Ismail M, et al (2019) Joint Planning of Smart EV Charging Stations and DGs in Eco-Friendly Remote Hybrid Microgrids. IEEE Trans Smart Grid 10:5819–5830. https://doi.org/10.1109/TSG.2019.2891900

Shafie-khah M, Heydarian-Forushani E, Osorio GJ, et al (2016) Optimal Behavior of Electric Vehicle Parking Lots as Demand Response Aggregation Agents. IEEE Trans Smart Grid 7:2654–2665. https://doi.org/10.1109/TSG.2015.2496796

Shlayan N, Challapali K, Cavalcanti D, et al (2018) A Novel Illuminance Control Strategy for Roadway Lighting Based on Greenshields Macroscopic Traffic Model. IEEE Photonics J 10:1–11. https://doi.org/10.1109/JPHOT.2017.2782801

Soroudi A, Aien M, Ehsan M (2012) A Probabilistic Modeling of Photo Voltaic Modules and Wind Power Generation Impact on Distribution Networks. IEEE Systems Journal 6:254–259. https://doi.org/10.1109/JSYST.2011.2162994

Spieker H, Hagg A, Gaier A, et al (2017) Multi-stage evolution of single- and multi-objective MCLP: Successive placement of charging stations. Soft Comput 21:4859–4872. https://doi.org/10.1007/s00500-016-2374-9

Sultana S, Roy PK (2015) Oppositional krill herd algorithm for optimal location of distributed generator in radial distribution system. International Journal of Electrical Power & Energy Systems 73:182–191. https://doi.org/10.1016/j.ijepes.2015.04.021

Wang G, Xu Z, Wen F, Wong KP (2013) Traffic-Constrained Multiobjective Planning of Electric-Vehicle Charging Stations. IEEE Trans Power Delivery 28:2363–2372. https://doi.org/10.1109/TPWRD.2013.2269142

Wei W, Wu D, Wu Q, et al (2019) Interdependence between transportation system and power distribution system: a comprehensive review on models and applications. J Mod Power Syst Clean Energy 7:433–448. https://doi.org/10.1007/s40565-019-0516-7

Wu Y, Xu C, Huang Y, Li X (2020) Green supplier selection of electric vehicle charging based on Choquet integral and type-2 fuzzy uncertainty. Soft Comput 24:3781–3795. https://doi.org/10.1007/s00500-019-04147-4

Xiong Y, Gan J, An B, et al (2018) Optimal Electric Vehicle Fast Charging Station Placement Based on Game Theoretical Framework. IEEE Trans Intell Transport Syst 19:2493–2504. https://doi.org/10.1109/TITS.2017.2754382

Yi T, Cheng X, Zheng H, Liu J (2019) Research on Location and Capacity Optimization Method for Electric Vehicle Charging Stations Considering User's Comprehensive Satisfaction. Energies 12:1915. https://doi.org/10.3390/en12101915

Zhang H, Tang L, Yang C, Lan S (2019a) Locating electric vehicle charging stations with service capacity using the improved whale optimization algorithm. Advanced Engineering Informatics 41:100901. https://doi.org/10.1016/j.aei.2019.02.006

Zhang Y, Zhang Q, Farnoosh A, et al (2019b) GIS-Based Multi-Objective Particle Swarm Optimization of charging stations for electric vehicles. Energy 169:844–853. https://doi.org/10.1016/j.energy.2018.12.062

Zheng Y, Dong ZY, Xu Y, et al (2014) Electric Vehicle Battery Charging/Swap Stations in Distribution Systems: Comparison Study and Optimal Planning. IEEE Trans Power Syst 29:221–229. https://doi.org/10.1109/TPWRS.2013.2278852

Figures

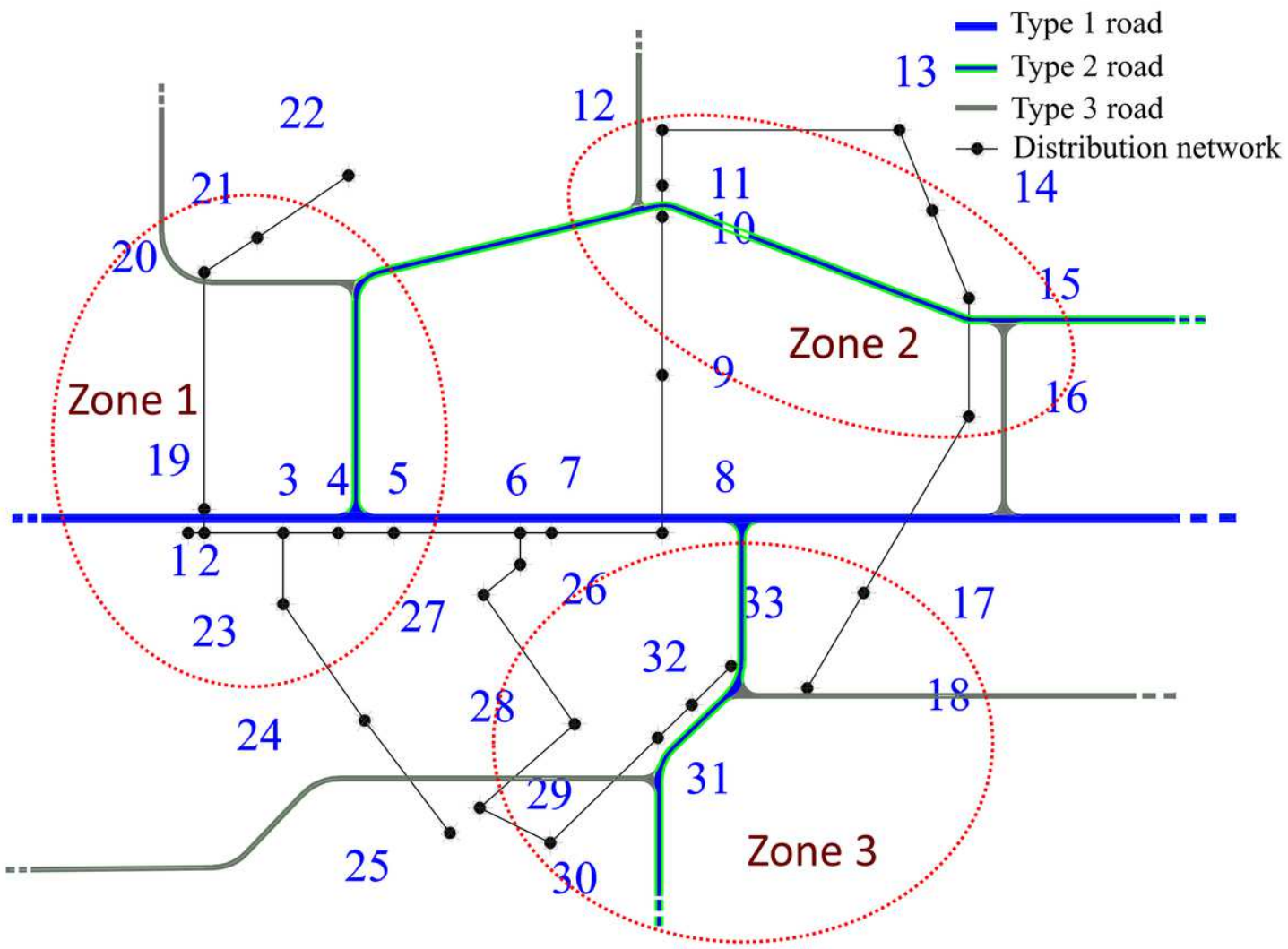

Figure 1

Superimposed study area with power distribution and traffic network.

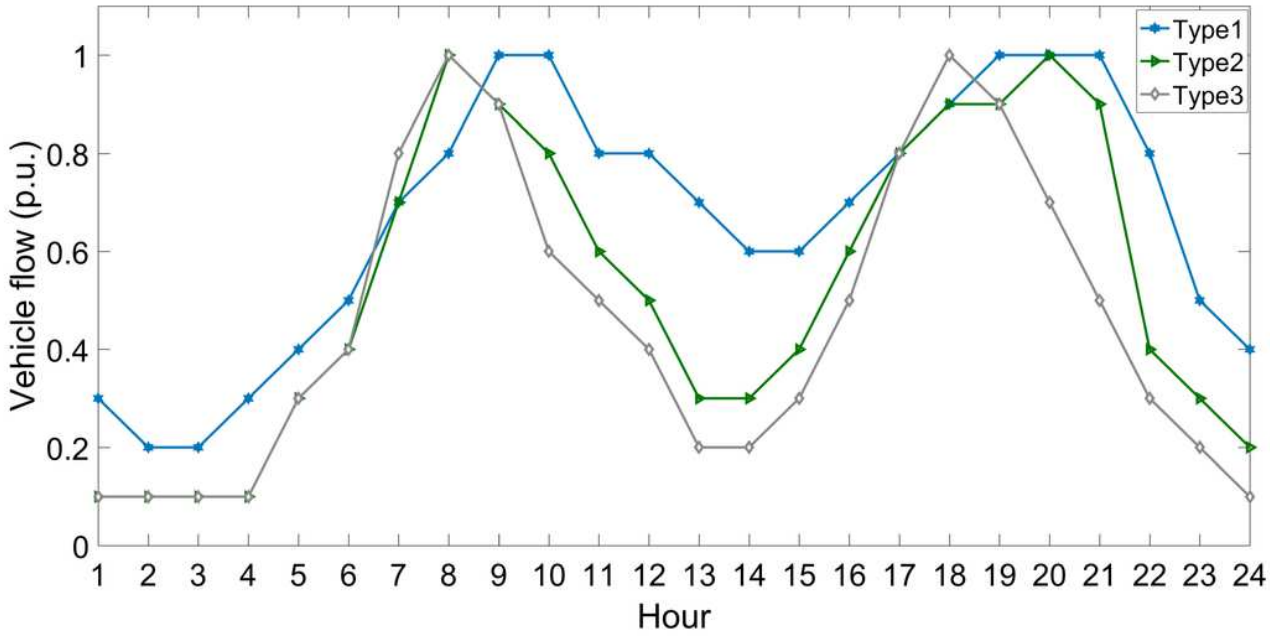

Figure 2

Annual average vehicle flow profile of three types of road.

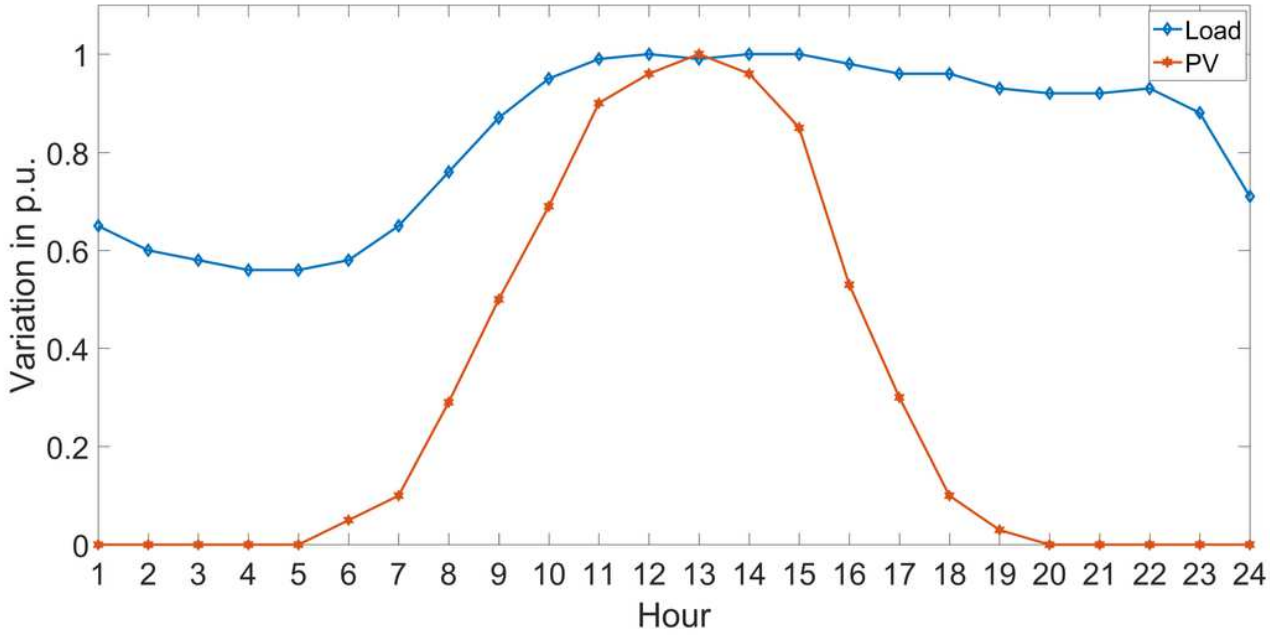

Figure 3

Annual average vehicle flow profile of three types of road (Pal et al. 2020).

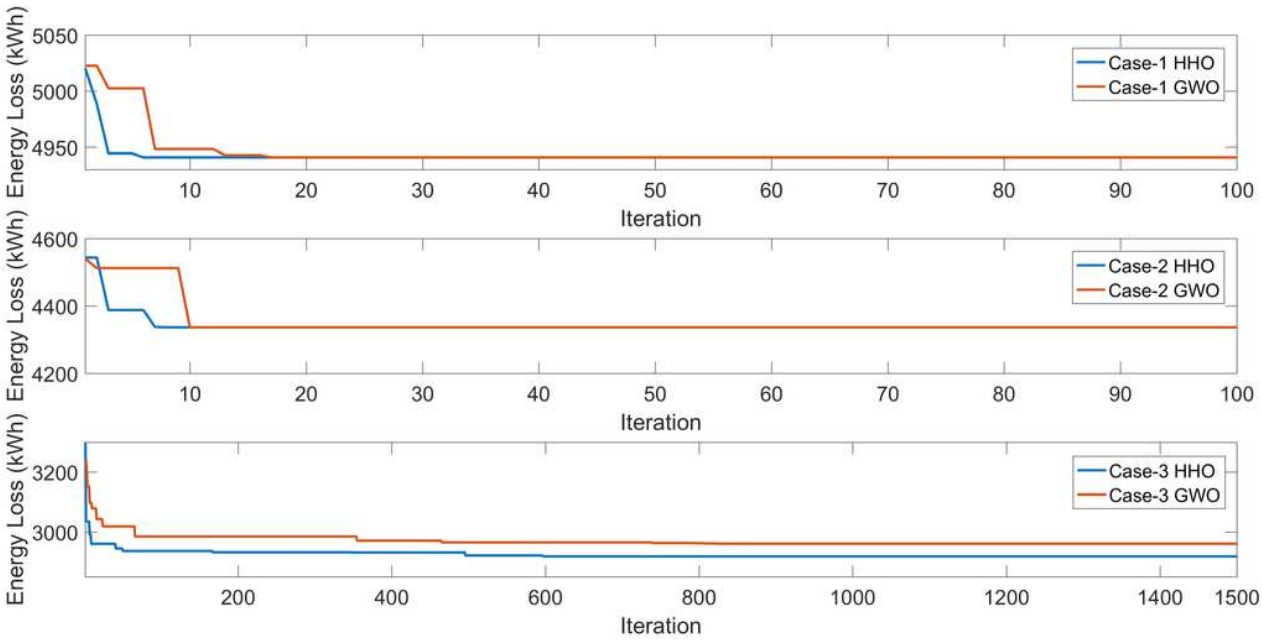

Figure 4

Convergence curves of GWO and HHO for case-1 to 3 with 100% EV penetration

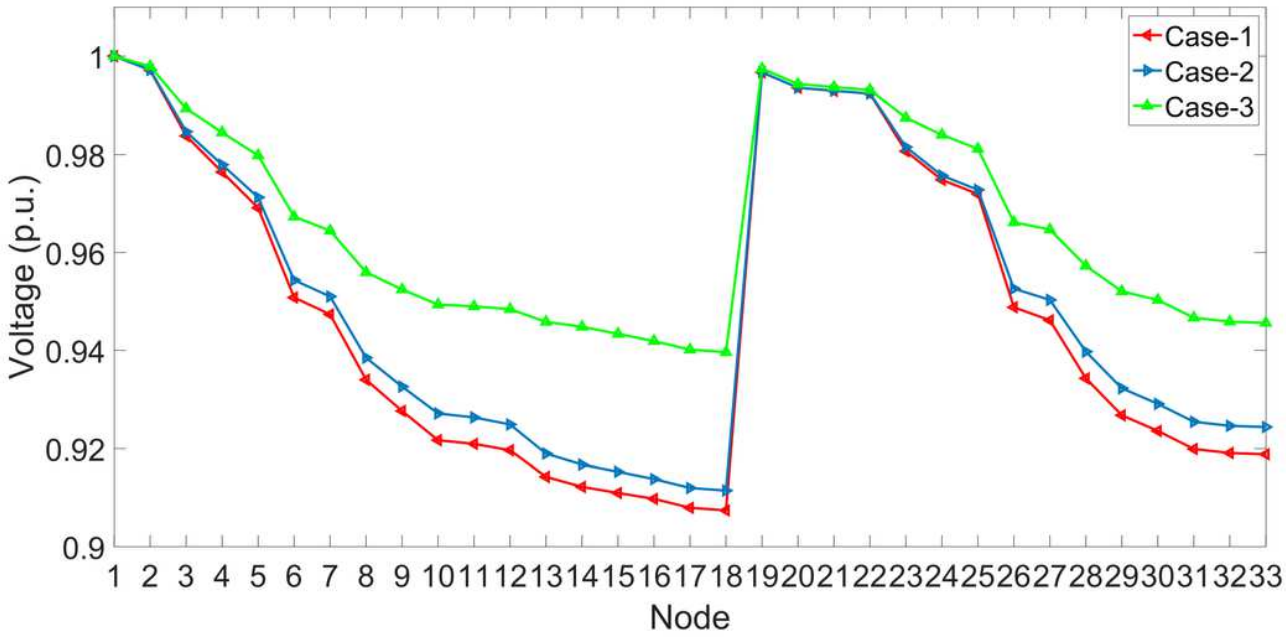

Figure 5

Daily average voltage profiles of the distribution network for case-1 to 3 with 100% EV penetration.

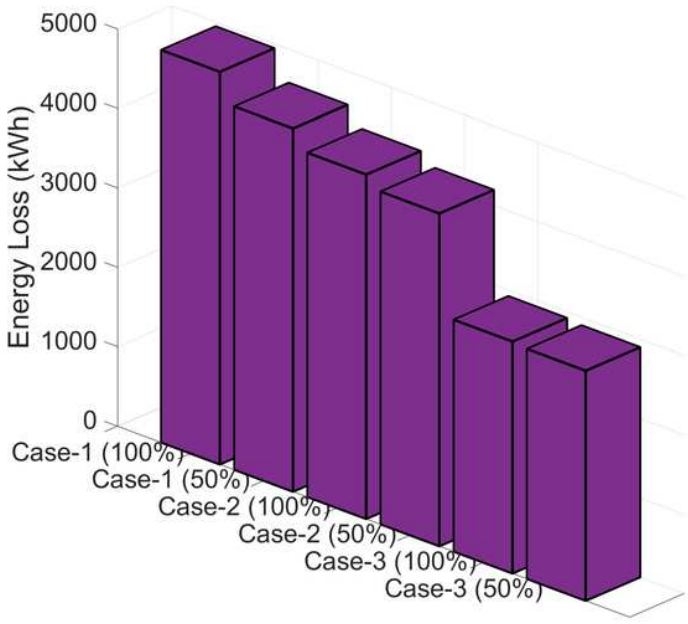

Figure 6

Comparison of all the cases with 100% and 50% EV penetration.

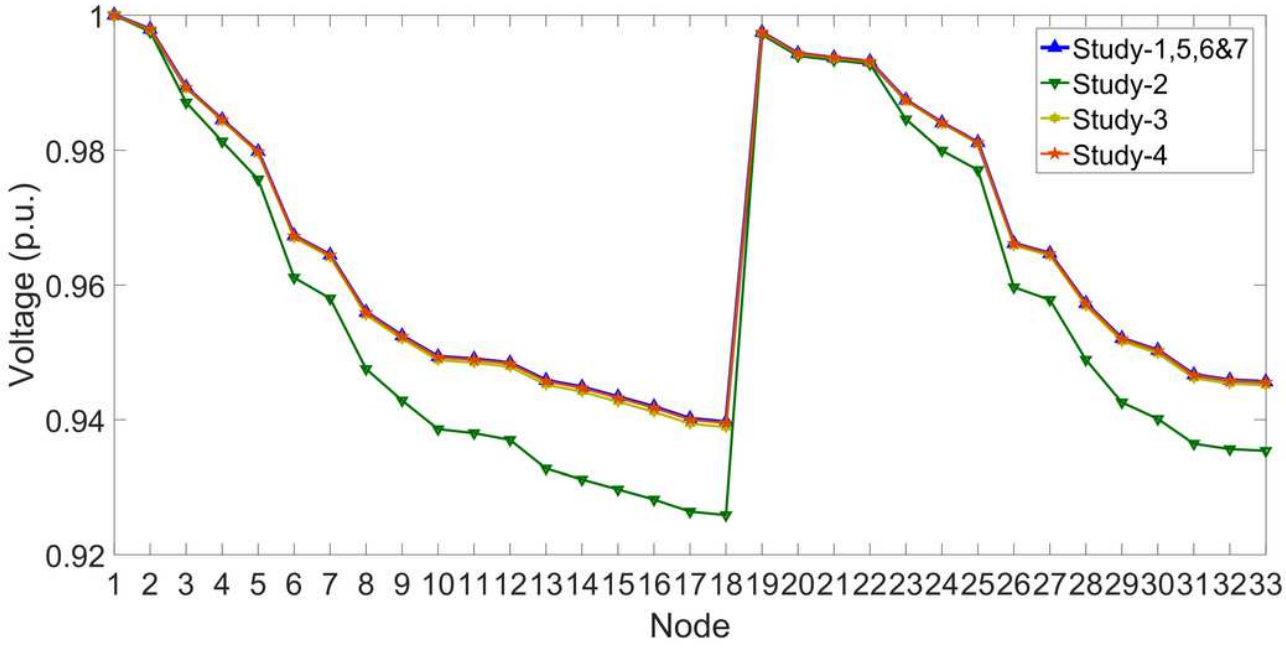

Figure 7

Daily average voltage profiles of different sensitivity studies.

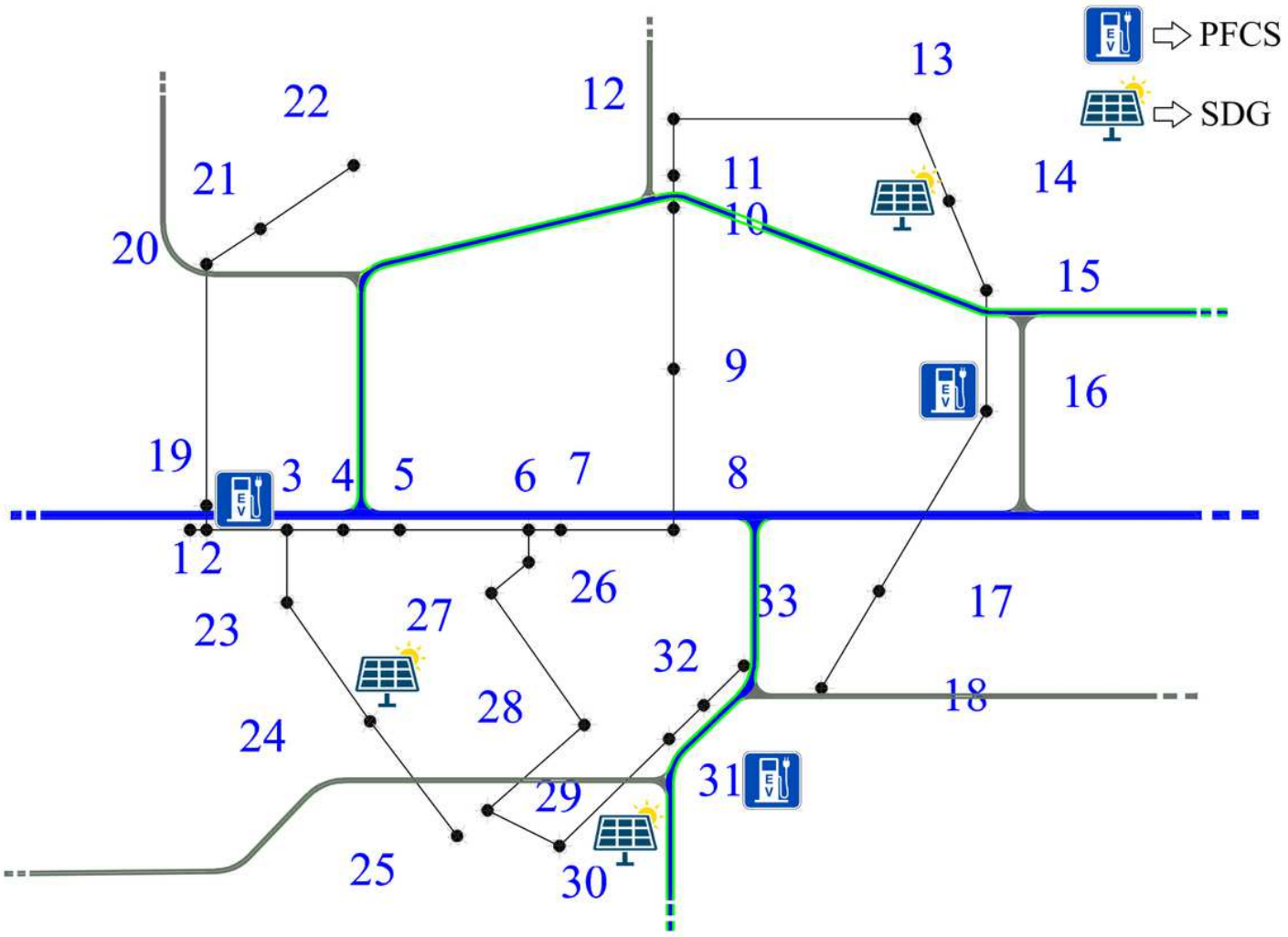

Figure 8

Allocation of PFCSs and SDGs.